





Reducing of Residual Stresses in Metal Parts Produced By SLM Additive Technology with Selective Induction Heating

Sergei A. Lychev¹  and Montaser Fekry^{2,3} 

¹ Institute for Problems in Mechanics, Russian Academy of Sciences, 101 Vernadsky Avenue, Bldg 1, Moscow 119526, Russia

lychevsa@mail.ru

² Department of Mechanics and Control Processes, Moscow Institute of Physics and Technology, Moscow, Russia

montaser.fekry@yahoo.com

³ Department of Mathematics, Faculty of Science, South Valley University, Qena, Egypt

Abstract. In the present paper a mathematical model for the temperature and residual stress fields evolution in growing thermoelastic cylinder is investigated. It is based on the idea of analyzing a sequence of boundary value problems describing the steps of the growth process. The main goal is to give qualitative clarification and modeling for residual stress accumulation and distortion in the final geometric shape, which appears in additive manufacturing, particularly in SLM or SLS technological processes. We proposed such way to control these unwanted phenomena. The main idea is to apply inhomogeneous inductive heating by skin effect phenomena during the additive process. In so doing one can compensate the incompatibility of thermoelastic deformations caused by sequential addition of heated up to melting temperature material by controlled inhomogeneous thermal expansion resulting from such way of heating. The process can be controlled by changing the frequency of an alternating electric current and the amplitude supplied to the growing body. This controlling leads to minimize residual stresses and/or shape distortion of the body during and after additive process completion. For the axisymmetric cylindrical problem investigated below, it is possible to obtain optimal control parameters based on analytical solution of sequence of boundary value problems. This solution is the main result of present paper.

Keywords: Additive manufacturing · Residual stresses · Growing solids · Thermoelasticity · Analytical solutions

1 Introduction

Selective Laser Melting and Sintering (SLM and SLS) are promising technology for manufacturing 3D metal parts with complicate shape and specified inhomogeneity. The main theme is that the part is being created sequentially, piece by piece, due to melting and fusing metallic powders together in precise geometric shape [1–4]. There are, nonetheless, some challenges that hamper the practical application of such technologies. One of the most tangible is related with inhomogeneous thermal expansion of added material in the course of technological process. The main reason behind the latter is that the metallic particles are heated to the melting temperature and then attached to manufactured component part, which temperature is less then the temperature of the particles. After temperature equalisation an incompatible deformations arise both in bulk of the body and attached part. This causes distortion of geometrical shape and accumulation of residual stresses.

Residual stresses can be defined as those stresses that remain in a material or body after manufacturing in the absence of external forces or thermal gradients. Residual stresses have the same effect on materials and their performance as externally applied stresses [5–12]. It leads to undesirable consequences, such as a shape distortion, local discontinuity, loss of stability.

Up to now a variety of ways to reduce residual stresses in SLM manufactured parts are known. Most use the modulation of melting beam or overall heating of the part during additive process [13–17]. These allow to reduce the inhomogeneity of temperature field and, consequently, to reduce residual stresses. In present work we propose to take a further step: to heat the part during SLM process in specific non-uniform manner which upon the technological (melting) heating results in almost constant temperature profiles and hence in low residual stresses. In order to generate such specific heating, an induction with high frequency current modulated in time can be used. One may observe here the similarity with skin-effect induced by alternating current.

2 Growing Process

The concept of a solids growth refers to a new branch of continuum mechanics [18–23], therefore it seems appropriate here to clarify the definition of the growing solid. In a broad sense growing process defines the alteration of the body composition occurring in the course of deformation. The growing process may be accompanied by a change of topological properties of the body. It can be said that the altering of the body composition is the accession of new material points and (or) formation of new constrains between particles already included into the composition. It should also be noted that the change of topological properties can occur without the influx of material and can be caused by the transition of the boundary points into the interior. In modern continuum mechanics there are many different approaches to the studying of the growth phenomenon. For today a large number of papers devoted to mechanics of growing solids have

been published. References may be found in the review [8]. The works [24,25] are devoted to the development of geometric methods adopted for the mechanics of incompatible strains arising as the result of the growing process. In the works [18–21] the growth is investigated as the continuous process of deposition of strained material surfaces to a deformable 3D body. It is known that under certain additional assumptions on the continuity of functions that define the stress-strain state of adhered material surfaces, the continuous growing process can be considered as the limit of a sequence of discrete processes [26,27].

A discretely accreted body is represented as a finite family of added layers to the initial body

$$\mathfrak{B}_0 \subset \mathfrak{B}_1 \subset \dots \subset \mathfrak{B}_k \subset \dots \subset \mathfrak{B}_N, \quad (1)$$

where \mathfrak{B}_0 is the initial body and \mathfrak{B}_k is \mathfrak{B}_0 after adding k layers. The sequence (1) is associated with the sequence of numbers

$$0 < \tau_1 < \dots < \tau_k < \dots < \tau_N, < \dots < \quad (2)$$

determining the accretion times, i.e. the times at which the layers $\mathfrak{B}_k \setminus \mathfrak{B}_{k-1}$, $k = 1, \dots, N$ are added to the body \mathfrak{B}_0 . The sequences (1) and (2) together determine the body growth scenario. In general case, the strain, temperature, and velocity fields of the assembly \mathfrak{B}_k are inconsistent with the fields of the assembly \mathfrak{B}_{k-1} . Therefore, the dynamic processes in the growing body vary by jump at the attachment times.

The process of dynamic discrete accretion can be modeled by successively solving the boundary value problems for the bodies \mathfrak{B}_k . Then the initial data for the step is determined by the values of the corresponding fields at the final time moment of the preceding one and by the values associated with the attached elements. Formally, the recursive sequence of problems in the linear approximation can be stated as follows:

$$\begin{aligned} \forall x \in \mathfrak{B}_0 \quad \mathcal{L}_0 \mathbf{u}_0 + \mathcal{B}^0 = 0, \quad \forall x \in \partial \mathfrak{B}_0 \quad \mathcal{D}_0 \mathbf{u}_0 = 0, \quad \mathbf{u}_0|_{t=0} = \mathbf{u}_0^0, \quad \dot{\mathbf{u}}_0|_{t=0} = \mathbf{v}_0^0, \\ \vdots \\ \forall x \in \mathfrak{B}_n \quad \mathcal{L}_n \mathbf{u}_n + \mathcal{B}_n^0 = 0, \quad \forall x \in \partial \mathfrak{B}_n \quad \mathcal{D}_n \mathbf{u}_n = 0, \quad \mathbf{u}_n|_{t=\tau_n} = 0, \quad \dot{\mathbf{u}}_n|_{t=\tau_n} = \mathbf{v}_n^0, \end{aligned}$$

$$\begin{aligned} \mathcal{B}_n^0 = \mathcal{B}_{n-1}^0 + \begin{cases} \mathcal{L}_{n-1} \mathbf{u}_{n-1}|_{t=\tau_n} & \text{for } x \in \mathfrak{B}_{n-1}, \\ 0 & \text{for } x \in \mathfrak{B}_n \setminus \mathfrak{B}_{n-1}, \end{cases} \\ \mathbf{v}_n^0 = \begin{cases} \dot{\mathbf{u}}_{n-1}|_{t=\tau_n} & \text{for } x \in \mathfrak{B}_{n-1}, \\ \mathbf{v}^0 & \text{for } x \in \mathfrak{B}_n \setminus \mathfrak{B}_{n-1}, \end{cases} \end{aligned}$$

here $\mathcal{L}_0, \dots, \mathcal{L}_n$ are differential operators determined by the same differential operation (the field equations) but in different domains, $\mathcal{D}_0, \dots, \mathcal{D}_n$ are operators of boundary conditions, \mathcal{B}^0 are external volume force and density of heat source, \mathbf{v}^0 are the velocities associated with the attached elements, and $\mathbf{u}_0, \dots, \mathbf{u}_n$ are

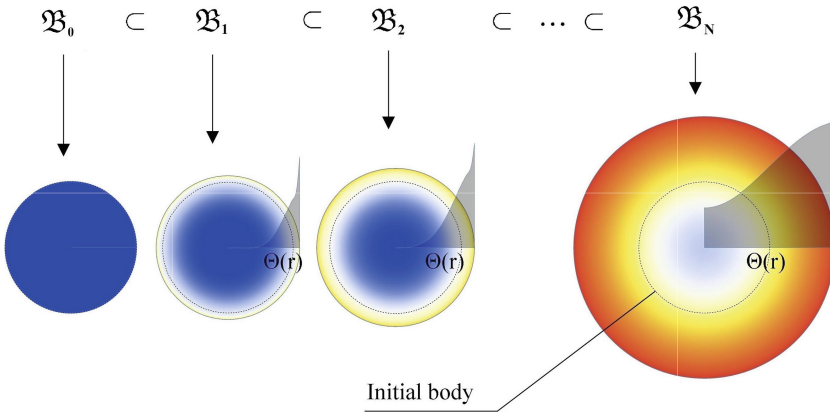


Fig. 1. Schematics for thermoelastic growing process.

increments of the displacement and temperature fields with respect to the beginning of the step. The dot denotes the derivative with respect to time, and $\mathbf{u}_0^0, \mathbf{v}_0^0$ are the initial data for the first step.

The schematics for thermoelastic growing process is shown on Fig. 1 . One can see on this figure the sequence of cylindrical cross sections for the first few steps and the final step of discrete growth. The coloured rendering denotes the temperature distribution which is also shown on inserted semi-transparent plots. All this illustration is based on analytical solution, set out later in the paper.

3 Initial-Boundary Problem at a Step

At the outset the analytical solution of the boundary value problem for the body at step k is obtained. To stay within the framework of the linear theory, it's supposed that the displacements and excess temperatures, as well as their gradients, are small.

The growing body is considered as a thermally and electrically conducting elastic cylinder $\mathcal{C} = \{(r, \theta, z) : 0 \leq r < R, 0 \leq z \leq L, 0 \leq \theta < 2\pi\}$, therefore the problem is formulated in the cylindrical coordinates (r, θ, z) , that are related to the Cartesian coordinates (x, y, z) as follows

$$r = \sqrt{x^2 + y^2}, \quad \theta = \tan^{-1} \frac{y}{x}, \quad z = z,$$

$$\mathbf{e}_r = \cos \theta \mathbf{i} + \sin \theta \mathbf{j}, \quad \mathbf{e}_\theta = -\sin \theta \mathbf{i} + \cos \theta \mathbf{j}, \quad \mathbf{e}_z = \mathbf{k},$$

where, $(\mathbf{e}_r, \mathbf{e}_\theta, \mathbf{e}_z)$ and $(\mathbf{i}, \mathbf{j}, \mathbf{k})$ are the basis of the cylindrical and Cartesian coordinates respectively.

3.1 Skin Effect

Here the skin effect phenomenon in a cylinder is briefly discussed, which can be obtained from Maxwell's equations [28,29]:

$$\begin{aligned} \nabla \cdot \mathbf{E} &= 0, & \nabla \times \mathbf{E} &= -\frac{\partial \mathbf{B}}{\partial t}, \\ \nabla \cdot \mathbf{B} &= 0, & \nabla \times \mathbf{B} &= \mu_0 \left(\mathbf{J} + \epsilon_0 \frac{\partial \mathbf{E}}{\partial t} \right). \end{aligned} \quad (3)$$

Here \mathbf{E} is the electric field, \mathbf{B} is the magnetic field, \mathbf{J} is the total electric current density per unit area, μ_0 is the permeability, and ϵ_0 is the electric permittivity.

With the assumption that the material is isotropic, the relation between current density \mathbf{J} , electrical conductivity σ and applied electric field \mathbf{E} can be written as

$$\mathbf{J} = \sigma \mathbf{E}. \quad (4)$$

Taking into account that for an ideal conductor $\frac{\partial \mathbf{E}}{\partial t} = 0$, and with the aid of constitutive relation (4), applying the curl operator to the second equation of (3). This results in

$$\nabla^2 \mathbf{J} - \mu_0 \sigma \dot{\mathbf{J}} = 0, \quad (5)$$

where

$$\nabla^2 = \frac{\partial^2}{\partial r^2} + \frac{1}{r} \frac{\partial}{\partial r}.$$

Consider time-harmonic AC current with angular frequency ω and amplitude phasor $\mathbf{J} = J e^{-i\omega t} \mathbf{e}_z$, where the current flows in the z direction. Under this assumption Eq.(5) reduces to

$$\frac{\partial^2 J}{\partial r^2} + \frac{1}{r} \frac{\partial J}{\partial r} + k^2 J = 0. \quad (6)$$

Here

$$k = \frac{1+i}{\delta}, \quad \delta = \sqrt{\frac{2}{\omega \mu_0 \sigma}}, \quad i = \sqrt{-1},$$

δ denotes the skin depth, which is defined as the depth below the surface of the conductor at which the current density has fallen to $1/e$ (about 0.37) of the total current.

To complete the boundary value problem, consider the boundary conditions

$$\mathbf{E} \cdot \mathbf{n}|_{r=R} = 0, \quad \int_c \mathbf{J} \cdot \mathbf{ds} = I, \quad \mathbf{ds} = r d\mathbf{e}_z,$$

where \mathbf{n} denotes unit normal to cylindrical part of the boundary and I is the total current.

The general solution of Eq.(6), which is bounded at $r = 0$, takes the form

$$J = C J_0(kr), \quad (7)$$

where $J_0(\cdot)$ is the Bessel function of the first kind and zero order.

One can obtain the value for constant C from the integral boundary condition

$$I = 2\pi \int_0^R C J_0(kr) r dr, \tag{8}$$

that relates total current with distribution of the current density.

From the following relation between Bessel functions

$$\frac{\partial}{\partial r} r^m J_m(r) = r^m J_{m-1}(r),$$

the integral (8) can be calculated in analytical form, therefore the solution (7), which expresses the distribution of alternating current in a cylinder of radius R , can be written as

$$J = \frac{kI}{2\pi R} \frac{J_0(kr)}{J_1(kR)}.$$

Figure 2 shows the alternating current density in the Copper cylinder for three different frequencies $\omega_3 > \omega_2 > \omega_1$,

$$\begin{aligned} \sigma &= 5.9 \times 10^7 \text{ S m}^{-1}, \quad \mu_0 = 1.256629 \times 10^{-6} \text{ H m}^{-1}, \\ \{\omega_1, \omega_2, \omega_3\} &= \{5, 7, 9\} \times 2\pi \times 10^5 \text{ s}^{-1}. \end{aligned}$$

According to the Joule-Lenz law, the power of heating generated by an electrical conductor is proportional to the product of its resistance and the square of the current, thus, the temperature in that conductor will be concentrated near the surface.

$$\varpi = \frac{1}{2\sigma} |\mathbf{J}|^2.$$

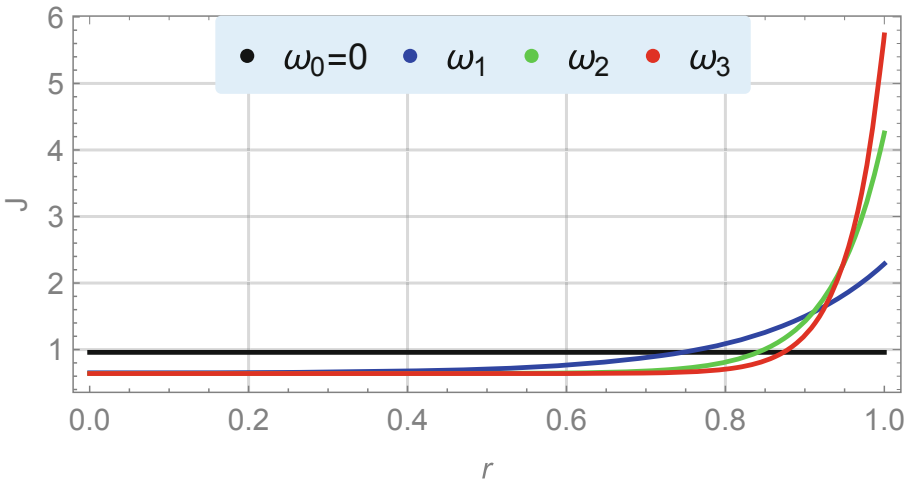


Fig. 2. The current density in cylinder with different frequencies.

3.2 Heat Transfer

The distribution of the temperature can be obtained from the solution of the heat conduction problem

$$\begin{aligned} \Lambda \nabla^2 \Theta - \rho \kappa \dot{\Theta} + \varpi^* &= 0, \\ \partial_r \Theta|_{r=R} &= 0, \quad \Theta|_{t=0} = \Theta_0, \end{aligned} \quad (9)$$

where Θ is the temperature change above the uniform reference temperature T_0 , ρ is the mass density, Λ is the coefficient of thermal conductivity, κ is the specific heat per unit mass at constant strain and ϖ^* is the heat source.

To facilitate the solution, the following non-dimensional variables are used

$$\check{r} = \frac{r}{R}, \quad \check{\Theta} = \frac{\Theta}{T_0}, \quad \check{t} = \frac{1}{R} \sqrt{\frac{\mu}{\rho}} t. \quad (10)$$

In the dimensionless variables (10), the equation (9) (after dropping the dimensionless symbol for simplicity) takes the form:

$$\nabla^2 \Theta - B \dot{\Theta} + \varpi = 0, \quad (11)$$

where the following dimensionless quantities are introduced

$$\varpi = \frac{R^2}{\Lambda T_0} \varpi^*, \quad B = \frac{\kappa R \sqrt{\mu \rho}}{\Lambda}.$$

The boundary and initial conditions in the dimensionless variables are stated as

$$\partial_r \Theta|_{r=\mathcal{R}} = 0, \quad \Theta|_{t=0} = \Theta_0.$$

Note that in the dimensionless form the radius of the initial cylinder takes the value “1”, and since the radius of the growing cylinder increases in a constant rate during the process we call the non-dimensional radius by \mathcal{R} .

With the Duhamel's principle [30], the solution of the heat equation (11) can be represented as the sum of particular solution Θ_p of the inhomogeneous equation and the solution Θ_h of the homogeneous one

$$\Theta = \Theta_h + \Theta_p.$$

The solution Θ_h meets the boundary value problem

$$\begin{aligned} \nabla^2 \Theta_h - B \dot{\Theta}_h &= 0, \\ \partial_r \Theta_h|_{r=\mathcal{R}} &= 0, \quad \Theta_h|_{t=0} = \Theta_0. \end{aligned} \quad (12)$$

By separation of variables one can get the solution for (12) as follows

$$\Theta_h = \bar{\Theta}(r) e^{-\frac{\gamma^2}{B} t}, \quad (13)$$

where $\bar{\Theta}$ is non-trivial solution of Sturm Liouville problem

$$\frac{\partial^2 \bar{\Theta}}{\partial r^2} + \frac{1}{r} \frac{\partial \bar{\Theta}}{\partial r} + \gamma^2 \bar{\Theta} = 0, \quad \partial_r \bar{\Theta}|_{r=1} = 0. \quad (14)$$

The bounded solution of eq. (14) at $r = 0$ (14) can be represented as follows

$$\bar{\Theta} = J_0(\gamma r),$$

The boundary condition at $r = \mathcal{R}$ gives a sequence values for γ

$$\gamma \in \{\gamma_m, m = 0, 1, \dots, \infty\},$$

where γ_m are the roots of the equation $J_1(\gamma\mathcal{R}) = 0$, here are some roots for $\mathcal{R} = 1$,

$$\{0, 3.83, 7.01, 10.17, 13.32, 16.47, 19.61, \dots\}.$$

Note: The first root of $J_1(\gamma\mathcal{R}) = 0$ is $\gamma_0 = 0$ and the other roots are numerically calculated in “*Mathematica*” by the order

$$\gamma_m = \frac{1}{\mathcal{R}} \text{BesselJZero}[1, m].$$

Thus, the non-trivial solutions (eigenfunctions) for Sturm Liouville problem (14) can be represented as follows

$$\bar{\Theta}_0 = 1, \quad \bar{\Theta}_m = J_0(\gamma_m r), \quad m, = 1, 2, \dots, \infty.$$

Due to the self-conjugate property of differential operator, defined with Eq. (14) and corresponding boundary conditions, all these solutions together constitute an orthogonal system. However, they are determined up to an arbitrary multipliers. It is appropriate to take them such that the system becomes normalized. To this end we calculate the normalization factors

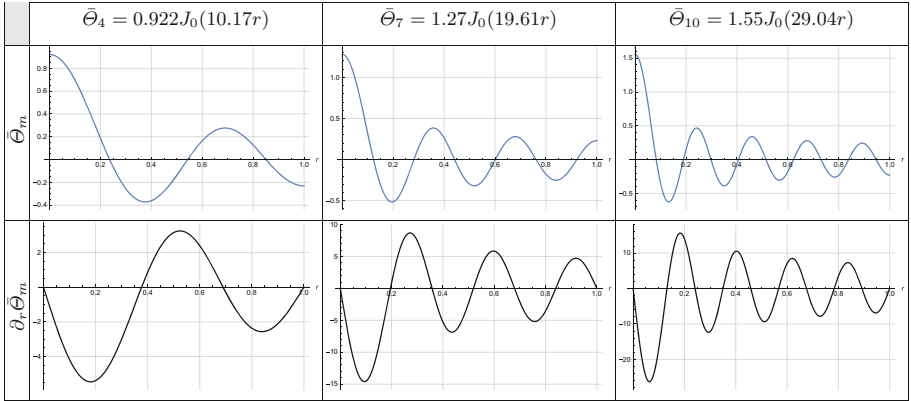
$$N_m = \sqrt{2\pi L \int_0^{\mathcal{R}} [J_0(\gamma_m r)]^2 r dr} = \mathcal{R}\sqrt{\pi L} |J_0(\gamma_m)|,$$

and divide solutions obtained above by them. Finally we get the orthonormal eigenfunctions system

$$\bar{\Theta}_0 = \frac{1}{\mathcal{R}\sqrt{\pi L}}, \quad \bar{\Theta}_m = \frac{J_0(\gamma_m r)}{\mathcal{R}\sqrt{\pi L} |J_0(\gamma_m)|}, \quad m, = 1, 2, \dots, \infty. \quad (15)$$

Table 1 shows graphs for three eigenfunctions with its derivatives with respect to r , it’s clear that solutions satisfy the boundary conditions.

Table 1. Some of eigenfunctions $\bar{\Theta}_m$ and their derivatives.



Now one can obtain the representation of solution for (12) in terms of expansion

$$\Theta_h = \sum_{m=0}^{\infty} C_m^h J_0(\gamma_m r) e^{-\frac{\gamma_m^2}{B} t}, \quad C_m^h = \frac{2\sqrt{\pi L}}{\mathcal{R}|J_0(\gamma_m)|} \int_0^{\mathcal{R}} \Theta_0 J_0(\gamma_m r) r dr. \quad (16)$$

With Dugamel’s principle one can obtain partial solution Θ_p for inhomogeneous problem (11) in such a way

$$\Theta_p = \sum_{m=0}^{\infty} J_0(\gamma_m r) \int_0^t C_m^p(s) e^{-\frac{\gamma_m^2}{B}(t-s)} ds, \quad C_m^p = \frac{2\sqrt{\pi L}}{J_0(\gamma_m)} \int_0^{\mathcal{R}} \varpi(r) J_0(\gamma_m r) r dr. \quad (17)$$

The sum of the series (16) and (17) provides formal solution for heat problem stated above. All elements in this representation except eigenvalues γ_m are obtained in closed form. In contrast with them the γ ’s are calculated numerically as the roots of transcendental equation. Some omissions may occur in their search that may cause the incompleteness for the solution. In this regard the verification is desirable at this stage.

To verify the completeness of eigenfunction-system and convergence of partial sum sequences we provide test expansions with “good and bad” examples. The former is the bump function, which is twice differentiable and obey boundary conditions stated above, and the latter is discontinuous function

$$G_1(r) = 64 \left(\frac{r}{\mathcal{R}}\right)^3 \left[1 - \frac{3r}{\mathcal{R}} + 3\left(\frac{r}{\mathcal{R}}\right)^2 - \left(\frac{r}{\mathcal{R}}\right)^3\right], \quad G_2(r) = \begin{cases} 1, & \frac{\mathcal{R}}{3} \leq r \leq \frac{2\mathcal{R}}{3} \\ 0, & \text{otherwise} \end{cases}.$$

The graphs for partial sums together with original functions are shown on Figs. 3 and 4. The sequences for corresponding Fourier coefficients are represented graphically on Fig. 5

As it can be seen from the figures, the partial sums of expansions for smooth function and for discontinuous function are significantly different, where convergence to the original smooth function is more satisfied even for small orders of partial sums. Thus, we numerically approve the completeness and convergency for proposed formal series.

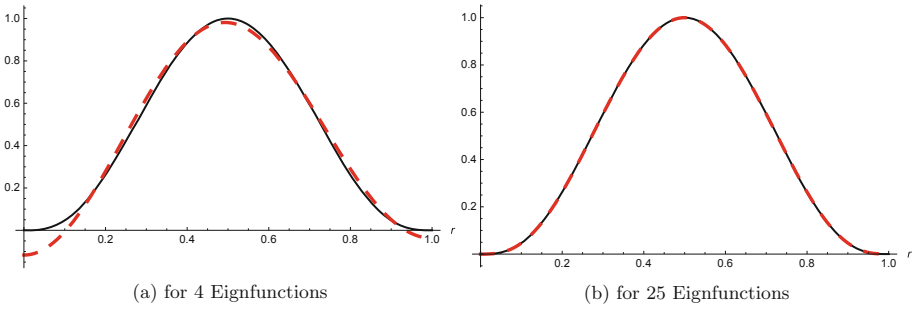


Fig. 3. Partial sums of different orders for the function $G_1(r)$.

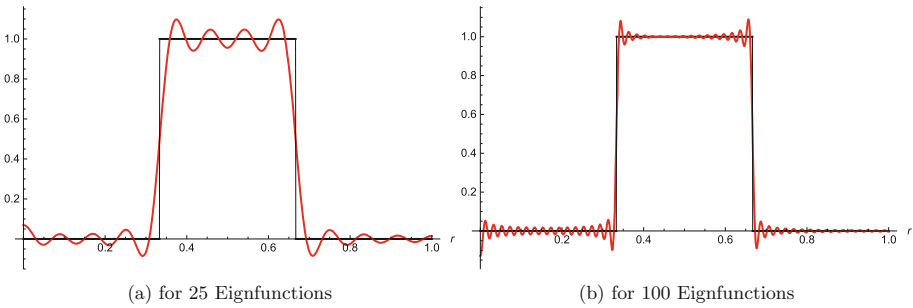


Fig. 4. Partial sums of different orders for the function $G_2(r)$.

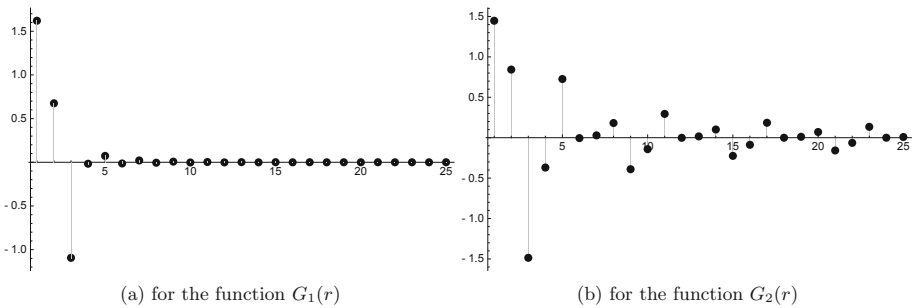


Fig. 5. Fourier coefficients for 25 corresponding eignfunctions.

3.3 Stress-Strain Problem

In the absence of body forces, the basic equations for temperature rate-dependent linear isotropic thermoelastic medium can be written as follows [31,32]:

$$\mu \nabla^2 \mathbf{u} + (\lambda + \mu) \nabla \nabla \cdot \mathbf{u} - \gamma \nabla \Theta = \rho \ddot{\mathbf{u}}, \quad (18)$$

where $\beta = (3\lambda + 2\mu)\alpha$, α is the coefficient of linear thermal expansion, λ and μ are Lamé's constants.

To facilitate the solution, the non-dimensional parameters (10) are used beside

$$\ddot{\mathbf{u}} = \frac{\mathbf{u}}{R}.$$

With dimensionless variables, the equations (18) (after dropping the dimensionless symbol for simplicity) takes the form:

$$\nabla^2 \mathbf{u} + k \nabla \nabla \cdot \mathbf{u} - A \nabla \Theta = \ddot{\mathbf{u}}, \quad (19)$$

where

$$k = \frac{\lambda + \mu}{\mu}, \quad A = \frac{\gamma T_0}{\mu}.$$

The boundary and initial conditions in the dimensionless form are stated as

$$\sigma_r|_{r=\mathcal{R}} = 0, \quad \mathbf{u}|_{t=0} = \mathbf{u}_0, \quad \dot{\mathbf{u}}|_{t=0} = \mathbf{v}_0,$$

the dimensionless stress components take the form

$$\sigma_r = (k - 1) \nabla \cdot \mathbf{u} + 2 \frac{\partial u}{\partial r} - A \Theta, \quad \sigma_\theta = (k - 1) \nabla \cdot \mathbf{u} + 2 \frac{u}{r} - A \Theta.$$

The separation of variables once again is used to solve the problem (18). Suppose that

$$\mathbf{u} = \mathbf{U}(r)\mathcal{T}(t).$$

In such a case Eq. (19) can be resolved to the form

$$[\nabla^2 \mathbf{U} + k \nabla \nabla \cdot \mathbf{U}] \mathcal{T} - \mathbf{U} \dot{\mathcal{T}} = \mathcal{X}, \quad (20)$$

where the notation $\mathcal{X} = \mathcal{X}(r, t) = A \nabla \Theta$ is introduced for brevity.

Now suppose that the following Sturm Liouville problem

$$\nabla^2 \mathbf{U} + k \nabla \nabla \cdot \mathbf{U} = -\eta^2 \mathbf{U}, \quad (21)$$

has solutions \mathbf{U}_i , $i = 1, 2, \dots, \infty$, which are corresponding to the eigenvalues η_i , $i = 1, 2, \dots, \infty$. Due to the fact that the differential operator, defined with Eq.(20) with the corresponding is self conjugate, the system of its eigenfunctions, that are the solutions of Sturm Liouville problem (21) is complete and orthonormal. After appropriate normalization it becomes orthonormal. We will

address this issue in more detail in next section. Here we suppose that such eigensystem is already known and one can obtain with it formal solution for (19), i.e.

$$\mathbf{u} = \sum_{i=1}^{\infty} \mathbf{U}_i(r) \mathcal{T}_i(t). \tag{22}$$

Using such a representation for \mathbf{u} the Eq. (20) can be transformed to

$$\sum_{i=1}^{\infty} [-\eta_i^2 \mathbf{U}_i \mathcal{T}_i - \mathbf{U}_i \ddot{\mathcal{T}}_i] = \mathcal{X}. \tag{23}$$

With the following notation for inner product

$$\langle \mathbf{U}_i, \mathbf{U}_j \rangle = 2\pi L \int_0^{\mathcal{R}} \mathbf{U}_i \cdot \mathbf{U}_j r dr = \begin{cases} 1 & i = j \\ 0 & i \neq j \end{cases},$$

one can get ordinary differential equations of the time variable t as follow

$$-\eta_j^2 \mathcal{T}_j - \ddot{\mathcal{T}}_j = \mathcal{Y}_j, \tag{24}$$

where

$$\mathcal{Y}_j(t) = \langle \mathbf{U}_j(r), \mathcal{X}(r, t) \rangle.$$

The initial conditions define the following relations

$$\begin{aligned} \mathbf{u}|_{t=0} &= \sum_{i=1}^{\infty} \mathbf{U}_i(r) \mathcal{T}_i(0) = \mathbf{u}_0, & \mathcal{T}_j(0) &= \langle \mathbf{U}_j, \mathbf{u}_0 \rangle = u_j^0, \\ \dot{\mathbf{u}}|_{t=0} &= \sum_{i=1}^{\infty} \mathbf{U}_i(r) \dot{\mathcal{T}}_i(0) = \mathbf{v}_0, & \dot{\mathcal{T}}_j(0) &= \langle \mathbf{U}_j, \mathbf{v}_0 \rangle = v_j^0. \end{aligned} \tag{25}$$

Finally, the general solution of the non-homogeneous equation (24) can be obtained as the sum of the solution of the corresponding homogeneous equation and a particular solution of the nonhomogeneous equation, i.e.

$$\mathcal{T}_j = u_j^0 \cos(\eta_j t) + \frac{v_j^0}{\eta_j} \sin(\eta_j t) - \frac{1}{\eta_j} \int_0^t \mathcal{Y}_j(s) \sin[\eta_j(t - s)] ds.$$

3.4 Eigenproblem

Keeping in mind, that all fields in considered problem depend only on radial coordinate r and time, we assume the dynamic displacement vector can be represented as $\check{\mathbf{u}} = \check{u} \mathbf{e}_r$. Then the Eq. (21), where $\mathbf{U} = U \mathbf{e}_r$, takes the form

$$\frac{\partial^2 U}{\partial r^2} + \frac{1}{r} \frac{\partial U}{\partial r} - \frac{U}{r^2} + \frac{\eta^2}{(k+1)} U = 0, \tag{26}$$

the solution of Eq. (26) can be represented in terms of Bessel function

$$U = c_1 J_1(ar), \quad a = \sqrt{\frac{\eta^2}{k+1}}, \tag{27}$$

where c_1 is arbitrary constant. Using the boundary conditions for the stresses on cylinder's surface, we obtain a homogeneous algebraic equation

$$a(k+1)J_0(ar) - \frac{2J_1(ar)}{r} = 0. \tag{28}$$

The roots of Eq. (28) form a sequence of eigenvalues η_q , $q = 1, \dots, \infty$.

The complete system of eigenfunctions can be given as following

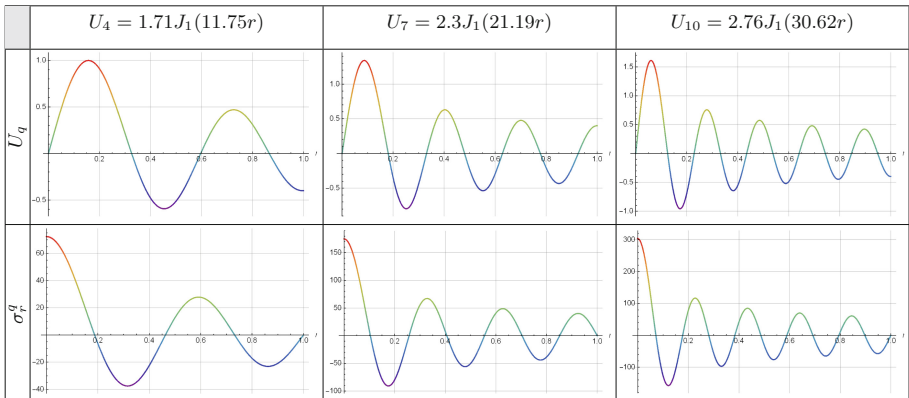
$$U_q = \frac{J_1(a_q r)}{\mathcal{N}_q}, \quad a_q = \sqrt{\frac{\eta_q^2}{k+1}},$$

where the normalization factor \mathcal{N}_q is given in the form

$$\mathcal{N}_q = \sqrt{2\pi L \int_0^{\mathcal{R}} J_1(a_q r)^2 r dr} = \left[\pi L \mathcal{R} \left(\mathcal{R} J_0(a_q)^2 - \frac{2J_0(a_q)J_1(a_q)}{a_q \mathcal{R}} + \mathcal{R} J_1(a_q)^2 \right) \right]^{\frac{1}{2}}.$$

Table 2 shows graphs for three eigenfunctions, which represent the displacement component in r direction, and the corresponding stress component σ_r^q , it's clear that solutions satisfy the boundary condition.

Table 2. Some of eigenfunctions U_q and their derivatives.



Test expansions of the eigenfunctions system U_q , for the discontinuous function $G2(r)$, which is mentioned in Subsect.(3.2) are provided. Figure 6 shows partial sums of different order.

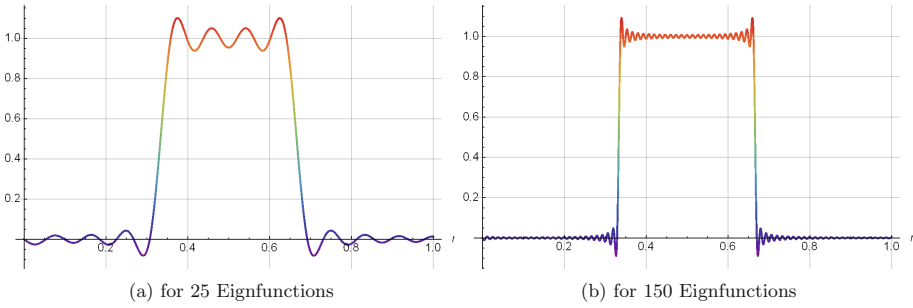


Fig. 6. Test expansion for different numbers of eigenfunctions.

From the stresses-displacement components relations, one can calculate the intensity of normal stresses τ , which is defined by the formula

$$\tau = \sqrt{\frac{1}{2}(\sigma_r - \sigma_\theta)^2}.$$

4 Computational Analysis and Discussion

In the rest of the paper we provide computational analysis for the thermoelastic growth of circular cylindrical solids, manufactured from one of the two metallic materials, copper which is diamagnetic, and titanium, purported to be paramagnetic.

The considered dimensions of the cylinder are radius $R = 0.5$ cm and length $L = 2$ cm. Calculations have been carried out with following material data [33,34]:

	λ, GPa	μ, GPa	$\rho, kg/m^3$	α, K^{-1}	$\Lambda, W/(mK)$	$\kappa, J/(kgK)$	$\sigma, S/m$	$\mu_0, H/m$
Titanium	113.8	44	4510	8.6×10^{-6}	17	521	2.38×10^6	1.26×10^{-6}
Copper	89.47	40.95	8960	16.4×10^{-6}	385	385	5.9×10^7	1.256629×10^{-6}

In a dimensionless form, the process starts at $r = 1$ as the radius of the initial cylinder, and then grows at 0.01, which represents the thickness of the new layer, every 4s (duration of a step).

It is assumed that there are no mass forces and at the initial time moment, the growing body was free from stresses and at rest.

In case of inhomogeneous heating, the metallic particles are heated to a temperature slightly lower than the melting temperature (the melting temperature of Copper and Titanium are 1360 K and 1940 K respectively) and then attached to the main part, which has temperature is less then the temperature of the particles, And because the body retains most of the heat during the process, the heat source must be controlled at every step as shown in Fig.7 so that the body does not melte complittly.

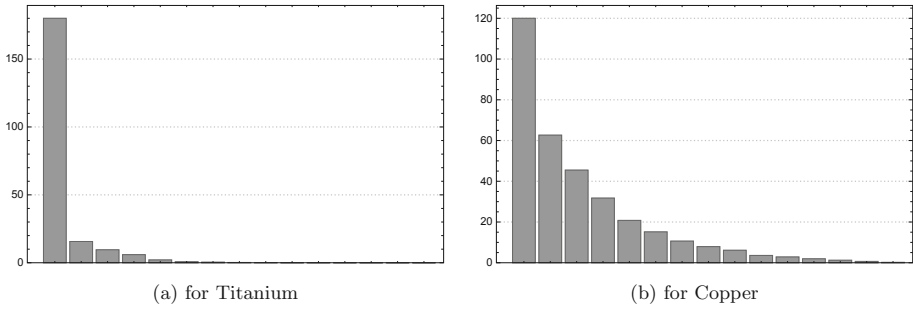


Fig. 7. The distribution of the heat source power during the process.

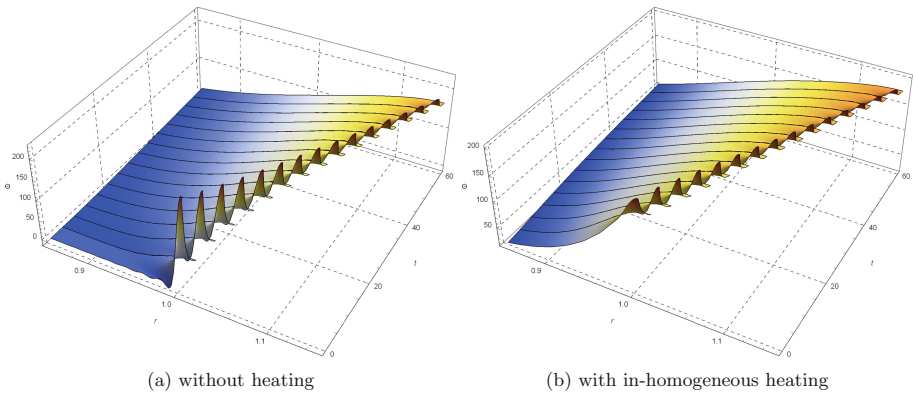


Fig. 8. The temperature distribution inside the body (Titanium).

Figures 8 and 9 show the temperature distribution in the whole body during the process for two cases: without heating and with external in-homogeneous heating of the growing body.

Figures 10 and 11 illustrate the temperature distribution on the moving boundary for the two cases. It's clear that, by using external heating, the gradient of temperature on the growing surface significantly decrease, thereby reducing residual stresses.

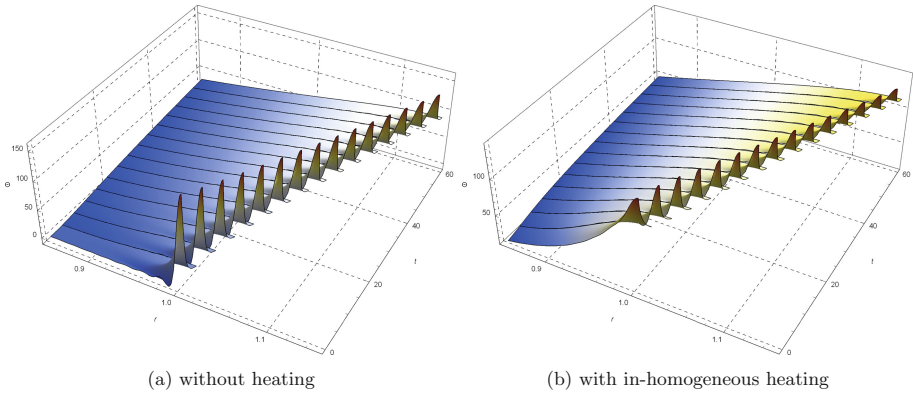


Fig. 9. The temperature distribution inside the body (Copper).

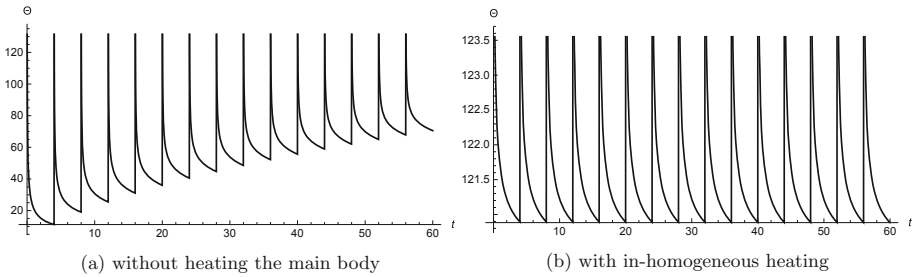


Fig. 10. The temperature distribution on the moving boundary for Copper.

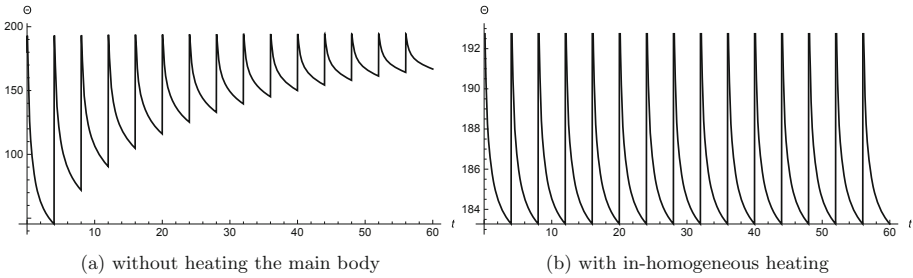


Fig. 11. The temperature distribution on the moving boundary for Titanium.

Figures 12 and 13 present the stress intensity distribution at some moment after ending the process for two cases: without heating and with external in-homogeneous heating of the growing body.

The main finding of the study can be outlined as follows. The inductive heating significantly affect on the residual stress distribution and being judiciously applied can substantially reduce them. The solution of corresponding optimiza-

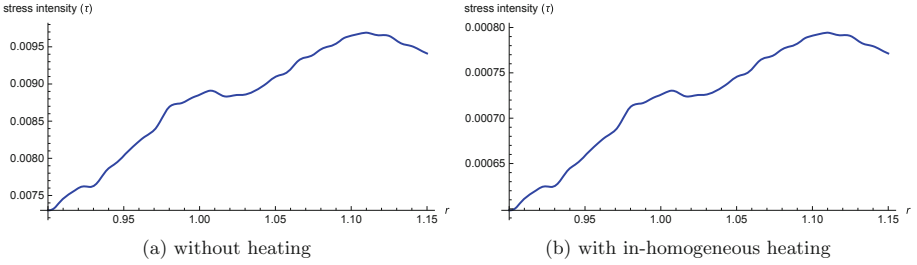


Fig. 12. The stress intensity distribution at some moment after ending the process for Copper.

tion problem are requested to determine the most viable option. This problem will be the subject of further research.

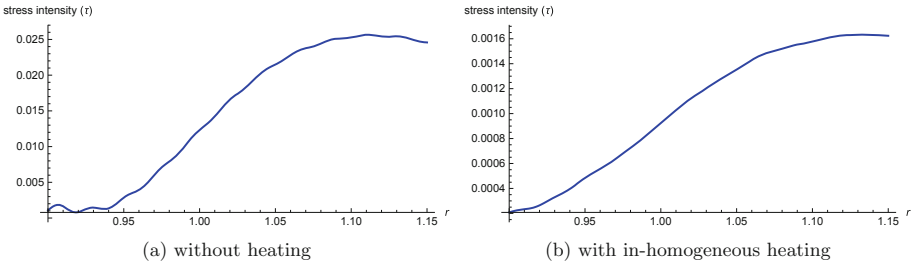


Fig. 13. The stress intensity distribution at some moment after ending the process for Titanium.

Acknowledgements. The study was partially supported by the Russian Government program (contract #AAAA – A20 – 120011690132 – 4) and partially supported by RFBR (grant No. 18 – 08 – 01346 and grant No.18 – 29 – 03228).

References

1. Levy, G.N., Schindel, R., Kruth, J.P.: Rapid manufacturing and rapid tooling with layer manufacturing (LM) technologies, state of the art and future perspectives. *CIRP Ann.* **52**(2), 589–609 (2003)
2. DebRoy, T., et al.: Additive manufacturing of metallic components-process, structure and properties. *Progress Mater. Sci.* **92**, 112–224 (2018)
3. Kruth, J.P., Leu, M.C., Nakagawa, T.: Progress in additive manufacturing and rapid prototyping. *CIRP Ann. Manuf. Technol.* **47**(2), 525–540 (1998)
4. Meiners, W., Wissenbach, K., Gasser, A.: Shaped body especially prototype or replacement part production. *DE Patent.* **19** (1998)
5. Ciarletta, P., Destrade, M., Gower, A.L., Taffetani, M.: Morphology of residually stressed tubular tissues: beyond the elastic multiplicative decomposition. *J. Mech. Phys. Solids* **90**, 242–53 (2016)
6. Green, A.E.: Thermoelastic stresses in initially stressed bodies. *Proc. Royal Soc. London. Ser. Math. Phys. Sci.* **266**(1324), 1–9 (1962)
7. Johnson, B.E., Hoger, A.: The use of a virtual configuration in formulating constitutive equations for residually stressed elastic materials. *J. Elast.* **41**(3), 177–215 (1995)
8. Klarbring, A., Olsson, T., Stalhand, J.: Theory of residual stresses with application to an arterial geometry. *Arch. Mech.* **59**(4–5), 341–64 (2007)
9. Ozakin, A., Yavari, A.: A geometric theory of thermal stresses. *J. Math. Phys.* **51**(3), 032902 (2010)
10. Sadik, S., Yavari, A.: Geometric nonlinear thermoelasticity and the time evolution of thermal stresses. *Math. Mech. Solids* **22**(7), 1546–87 (2017)
11. Wang, J., Slattery, S.P.: Thermoelasticity without energy dissipation for initially stressed bodies. *Int. J. Math. Math. Sci.* **31**, 329–337 (2002)
12. Othman, M.I., Fekry, M., Marin, M.: Plane waves in generalized magneto-thermo-viscoelastic medium with voids under the effect of initial stress and laser pulse heating. *Struct. Eng. Mech.* **73**(6), 621–9 (2020)
13. Mercelis, P., Kruth, J.P.: Residual stresses in selective laser sintering and selective laser melting. *Rapid Prototyping J.* (2006)
14. Buchbinder, D., Meiners, W., Pirch, N., Wissenbach, K., Schrage, J.: Investigation on reducing distortion by preheating during manufacture of aluminum components using selective laser melting. *J. Laser Appl.* **26**(1), 012004 (2014)
15. Zaeh, M.F., Branner, G.: Investigations on residual stresses and deformations in selective laser melting. *Prod. Eng.* **4**(1), 35–45 (2010)
16. Vilaro, T., Colin, C., Bartout, J.D.: As-fabricated and heat-treated microstructures of the Ti-6Al-4V alloy processed by selective laser melting. *Metall. Mater. Trans. A.* **42**(10), 3190–3199 (2011)
17. Kruth, J.P., Deckers, J., Yasa, E., Wauthlé, R.: Assessing and comparing influencing factors of residual stresses in selective laser melting using a novel analysis method. *Proc. Inst. Mech. Eng. Part B J. Eng. Manuf.* **226**(6), 980–91 (2012)
18. Arutyunyan, N.K., Drozdov, A.D., Naumov, V.E.: Mechanics of growing viscoelastoplastic bodies (1987)

19. Lychev, S.A., Manzhirov, A.V.: The mathematical theory of growing bodies. Finite deformations. *J. Appl. Math. Mech.* **77**(4), 421–32 (2013)
20. Lychev, S.A., Manzhirov, A.V.: Reference configurations of growing bodies. *Mech. Solids* **48**(5), 553–560 (2013). <https://doi.org/10.3103/S0025654413050117>
21. Lychev, S.A.: Universal deformations of growing solids. *Mech. Solids* **46**(6), 863–76 (2011)
22. Lychev, S., Manzhirov, A., Shatalov, M., Fedotov, I.: Transient temperature fields in growing bodies subject to discrete and continuous growth regimes. *Procedia IUTAM*. **1**(23), 120–129 (2017)
23. Polyanin, A.D., Lychev, S.A.: Decomposition methods for coupled 3D equations of applied mathematics and continuum mechanics: partial survey, classification, new results, and generalizations. *Appl. Math. Mod.* **40**(4), 3298–324 (2016)
24. Lychev, S., Koifman, K.: *Geometry of Incompatible Deformations: Differential Geometry in Continuum Mechanics*. De Gruyter (2018)
25. Yavari, A.: A geometric theory of growth mechanics. *J. Nonlinear Sci.* **20**(6), 781–830 (2010)
26. Lychev, S.A., Manzhirov, A.V.: Discrete and continuous growth of hollow cylinder. Finite deformations. In: *Proceedings of the World Congress on Engineering*, vol. 2, pp. 1327–1332 (2014)
27. Levitin, A.L., Lychev, S.A., Manzhirov, A.V., Shatalov, M.Y.: Nonstationary vibrations of a discretely accreted thermoelastic parallelepiped. *Mech. Solids* **47**(6), 677–89 (2012)
28. Lorrain, P., Corson, D.R.: *Electromagnetic Fields and Waves* (1970)
29. Weeks, W.L.: *Transmission and distribution of electrical energy*, Harpercollins, (1981)
30. John, F.: *Partial Differential Equations*, Springer-Verlag. New York (1982)
31. Nowacki, W.: *Theory of Elasticity* [in Polish]. PWN, Warszawa (1970)
32. Othman, M.I., Fekry, M.: The effect of initial stress on generalized thermoviscoelastic medium with voids and temperature-dependent properties under Green-Neghdi theory. *Mech. Mech. Eng.* **21**(2), 291–308 (2017)
33. Lychev, S.A., Manzhirov, A.V., Joubert, S.V.: Closed solutions of boundary-value problems of coupled thermoelasticity. *Mech. Solids* **45**(4), 610–23 (2010)
34. Donachie, M.J.: *Titanium: a Technical Guide*. ASM International (2000)